Comparative Analysis of Pressure Sensors for Real-Time Diagnostics in Industrial Cyber-Physical Systems

Azamatjon Muhammadjonov[1], Akmaljon Mamatov[1], Yusufjon Mamasodikov[1], Umida Khusanova[1], Zulfiya Mamasodikova[1], Ibrokhimjon Khasanov[1], Jamshidbek Obidov[1], Umida Madmarova[1], Saodatkhon Isroilova[1] and Tayr Moydunov[2]

[1]*Fergana State Technical University, Fergana street 86, 150100 Fergana, Uzbekistan*

[2]*Osh Technological University, Nasirdin Isanov Street 81, 723503 Osh, Kyrgyzstan*

m.azamatjon0212@gmail.com, akmaljon9790011@gmail.com, yusufjonmamasodikov@gmail.com, manzura.chkam.umida86@gmail.com, mamasadikov52@bk.ru, ibroximjon.xasanov@fstu.uz, jamshidobidov19@gmail.com, u.madmarova3306@gmail.com, saodatxon.ferpi@gmail.com, tayr.moydunov@mail.ru

Keywords: Industrial Cyber-Physical Systems, Pressure Sensors, MEMS, Strain Gauge, Real-Time Diagnostics, Raspberry Pi.

Abstract: Industrial Cyber-Physical Systems (ICPS) require reliable and fast-response sensing solutions to ensure safe and efficient operation of industrial processes. Among various physical parameters, pressure plays a critical role in monitoring pneumatic, hydraulic, and fluid-based systems. This paper presents a comparative experimental study of two widely used sensing approaches for real-time diagnostics: a MEMS-based digital pressure sensor (BMP388) and a strain-gauge-based measurement system using the HX711 analog-to-digital converter. Laboratory experiments were conducted using a Raspberry Pi-based data acquisition platform under controlled conditions. Sensor performance was evaluated in terms of measurement accuracy, response time, signal stability, noise sensitivity, and integration complexity. Experimental results demonstrate that the BMP388 sensor provides higher accuracy and faster dynamic response, making it suitable for precision real-time diagnostics, while the HX711-based solution offers acceptable performance for force- and load-related monitoring tasks after calibration. The findings provide practical guidance for selecting pressure sensing solutions in industrial cyber-physical systems and highlight the feasibility of low-cost embedded platforms for industrial diagnostics.

1 INTRODUCTION

Industrial Cyber-Physical Systems (ICPS) have become a fundamental component of modern industrial infrastructures, enabling the seamless integration of physical processes with computational intelligence, embedded control systems, and communication networks. By combining sensing, data acquisition, real-time analytics, and automated decision-making mechanisms, ICPS architectures provide a unified framework for monitoring and controlling complex industrial environments. These systems are widely adopted in manufacturing, energy generation and distribution, transportation systems, oil and gas facilities, and process industries, where continuous monitoring and real-time decision-making are essential for maintaining operational reliability, safety, and efficiency.

A critical capability of ICPS is the implementation of accurate and reliable real-time diagnostics. Diagnostic subsystems rely heavily on sensor-generated data to evaluate system health, identify abnormal operating conditions, detect early-stage faults, and support predictive maintenance strategies. Timely and precise diagnostic information enables proactive interventions, reduces downtime, minimizes maintenance costs, and enhances overall system resilience. Within this context, the quality and reliability of sensor data directly influence the effectiveness of diagnostic algorithms and intelligent control strategies.

Among various measurable physical parameters, pressure represents one of the most informative and widely monitored quantities in industrial environments. Pressure variations directly reflect the operational condition of hydraulic, pneumatic, and fluid-based components, including pipelines, compressors, pumps, valves, actuators, and storage vessels. Abnormal pressure behavior may indicate leakage, blockage, cavitation, mechanical wear, or control system malfunction. Therefore, accurate pressure sensing is not only important for process optimization but also crucial for safety assurance and fault prevention.

Pressure sensors are extensively deployed across industrial systems to monitor and regulate fluid dynamics and mechanical loads. However, industrial environments impose stringent performance requirements on sensing devices. These requirements include high measurement accuracy, fast dynamic response, stability under varying load conditions, long-term reliability, and robustness against environmental disturbances such as temperature fluctuations, mechanical vibration, humidity, and electromagnetic interference. Furthermore, in the context of ICPS, sensors must be compatible with digital communication protocols and embedded processing platforms to enable real-time data transmission and analysis [1].

Different pressure sensing technologies-such as MEMS-based digital sensors and strain-gauge-based measurement systems-exhibit distinct operational principles and performance characteristics. Variations in sensitivity, noise immunity, dynamic behavior, calibration requirements, and integration complexity may significantly influence their suitability for specific diagnostic applications. Consequently, selecting an appropriate sensing architecture requires not only understanding its standalone specifications but also evaluating its behavior within a complete cyber-physical system framework [2].

Despite the broad application of pressure sensors in industrial systems, existing research frequently concentrates on individual sensor technologies, theoretical modeling, or isolated laboratory evaluations. Comparative investigations that assess multiple sensing approaches under identical acquisition conditions and within embedded cyber-physical architectures remain relatively limited. In particular, there is a lack of systematic studies that analyze how different pressure sensing configurations perform under real-time diagnostic conditions typical of industrial ICPS environments, including aspects of data acquisition, processing latency, and integration with embedded platforms. This study aims to address this gap by conducting a structured comparative analysis of two widely used sensing approaches for real-time diagnostics in industrial cyber-physical systems. The investigation evaluates key performance indicators such as measurement accuracy, response speed, signal stability, noise sensitivity, and integration capability with digital monitoring platforms. By examining both direct digital pressure sensing and indirect force-based measurement architectures under controlled and reproducible conditions, the research provides practical insights into their relative strengths and operational limitations [3].

The results of this study offer technical guidance for selecting appropriate pressure sensing solutions to enhance diagnostic reliability, system efficiency, and integration feasibility in industrial ICPS applications. Moreover, the findings contribute to the broader understanding of how low-cost embedded platforms can support scalable and effective real-time monitoring infrastructures.

The main contributions of this work are summarized as follows: A structured comparative evaluation of direct MEMS-based digital pressure sensing and indirect strain-gauge load-based measurement under identical embedded acquisition conditions. Quantitative assessment of measurement accuracy, short-term stability, and dynamic response using statistical validation (mean and standard deviation analysis with N = 100 samples per test point). Experimental characterization of architectural trade-offs between direct digital pressure sensing and indirect force-based monitoring within industrial cyber-physical systems. Implementation and validation of a low-cost Raspberry Pi-based real-time diagnostic platform for comparative sensor evaluation. Practical guidelines for selecting sensing architectures based on diagnostic requirements, dynamic behavior, and integration complexity.

The remainder of this paper is structured as follows: Section 2 describes the methodology and experimental setup, Section 3 presents the comparative results, Section 4 discusses the implications of the findings, and Section 5 concludes the paper with recommendations and directions for future research [4].

2 METHODS

This study employs a controlled comparative experimental methodology to evaluate two sensing approaches commonly used in industrial cyber-physical system (ICPS) diagnostics:

- a MEMS-based digital pressure sensor (BMP388),
- a strain-gauge-based load measurement chain using an HX711 analog-to-digital converter.

Unlike broad multi-technology surveys, this research focuses specifically on the practical integration and real-time performance comparison of these two low-cost sensing architectures under identical acquisition conditions. This targeted scope ensures methodological consistency and experimental reproducibility.

Experimental Platform. All experiments were conducted using a Raspberry Pi 4 Model B as the central data acquisition and processing unit. The BMP388 sensor was connected via the I²C interface. The HX711 module was interfaced using a two-wire serial communication protocol (DOUT, SCK). Data acquisition was performed at a fixed sampling rate of 100 Hz to ensure sufficient resolution for dynamic response analysis [5].

MEMS Pressure Measurement Procedure. The BMP388 sensor was evaluated under controlled laboratory conditions at near-atmospheric pressure levels. Static pressure increments were applied using a calibrated reference barometric standard. The reference instrument uncertainty was ±5 Pa [6].

Five discrete pressure points within the range 101325–102300 Pa were tested. For each test point:

- 100 consecutive samples were recorded,
- mean and standard deviation were calculated,
- response time was measured as the time required to reach 90% of the final value after a pressure step.

Temperature was maintained at 25 ± 1°C to minimize thermal drift effects.

Strain Gauge Measurement Procedure. The HX711 module was evaluated using a strain-gauge load cell under static load conditions. Known calibrated masses (1–5 kg) were sequentially applied. The conversion from force to pressure was not directly implemented; therefore, this configuration represents indirect load-based monitoring rather than direct pressure sensing. Prior to testing, a two-point calibration procedure was performed to determine the calibration coefficient K_{cal}, which defines the linear relationship between the measured ADC output voltage and the corresponding applied force.K_{cal}. For each load level:

- 100 samples were acquired,
- mean measurement error was calculated,
- signal stability was assessed through standard deviation analysis [7].

Performance Evaluation Criteria. Sensor performance was evaluated according to: Measurement accuracy (mean absolute error), Standard deviation (signal stability), Response time (ms), Noise sensitivity, Integration complexity. All data processing was performed using Python-based acquisition scripts executed on the Raspberry Pi platform [8].

3 RESEARCH RESULTS

The BMP388 is a micro-electro-mechanical systems (MEMS) pressure sensor that operates based on the deformation of a micromachined silicon diaphragm. When external pressure is applied, the diaphragm undergoes mechanical deformation, resulting in a measurable change in electrical parameters within the sensor structure. This change is internally converted into a digital pressure value using on-chip signal conditioning and analog-to-digital conversion.
The pressure measurement can be expressed as:

$$P = P_0 + \Delta P \qquad (1)$$

where P is the measured pressure, P_0 is the reference pressure, and ΔP represents the pressure-induced variation due to diaphragm deformation. In 1-formula, the measured pressure is expressed as the sum of a reference pressure and the pressure variation caused by diaphragm deformation under external load. For real-time applications, the digital output pressure value is obtained after internal compensation:

$$P_{out} = f(\Delta C, T) \qquad (2)$$

where ΔC is the change in capacitance caused by diaphragm deformation, and T denotes temperature compensation. In 2-formula, the output pressure is obtained through an internal conversion function that relates the capacitance change due to mechanical deformation with temperature compensation [9]. Strain gauge pressure sensors operate by converting mechanical stress into a change in electrical resistance. When pressure is applied to the sensor diaphragm, the bonded strain gauges experience deformation, causing a proportional resistance change. These changes are arranged in a Wheatstone bridge configuration to produce a differential voltage output. The relationship between strain and resistance change is given by:

$$\frac{\Delta R}{R} = GF * \varepsilon \qquad (3)$$

where ΔR is the resistance change, R is the nominal resistance, GF is the gauge factor, and ε is the mechanical strain. In 3-formula, the proportional relationship between mechanical strain and the resulting change in electrical resistance of the strain gauge element is defined. The output voltage of the Wheatstone bridge is:

$$V_{out} = V_{exc} \cdot \frac{\Delta R}{R} \quad (4)$$

In 4-formula, the Wheatstone bridge converts resistance variations into a measurable output voltage proportional to the applied pressure. The HX711 module amplifies and digitizes this low-level signal, producing a digital output proportional to the applied pressure:

$$P_{out} = K\_cal \cdot V_{out} \quad (5)$$

where $K_{cal}$is the experimentally determined calibration coefficient obtained through two-point linear calibration. In 5-formula, the digitized output pressure is calculated using a calibration coefficient that maps the measured voltage to the actual pressure value.

Cross-sectional view of the BMP388 pressure sensor. The Bosch BMP388 is a compact digital pressure and temperature sensor based on MEMS technology. In the cross-sectional illustration, the MEMS diaphragm, capacitive sensing element, signal conditioning ASIC, and the protective layer are visible. The sensor converts external pressure variations into a digital I²C/SPI output. [10]. Under the controlled laboratory conditions of this study, small deviations relative to the reference instrument were observed; however, these deviations represent short-term repeatability within a narrow measurement range rather than the specified absolute accuracy of the sensor. The sensor is widely used in drones, sports devices, and weather monitoring applications (Fig.1).

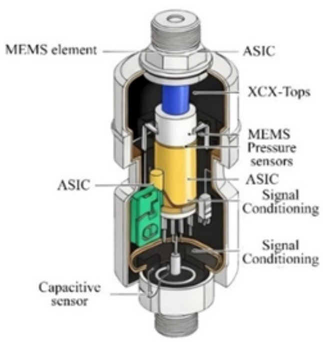

Figure 1: Digital MEMS-Based Pressure Sensor BMP388 Setup for Real-Time Industrial Cyber-Physical Systems.

External view of the HX711 module. The HX711 is a compact 24-bit sigma-delta analog-to-digital converter (ADC) primarily designed for measuring load cells and other differential analog signals. In the illustration, the central chip (HX711 IC), differential input pins, adjustable gain, internal clock generator, and simple two-wire serial output interface (DOUT and SCK) are clearly visible. The module is widely used with microcontrollers (Arduino, ESP32, etc.) in force, pressure, and weight measurement systems (Fig. 2).

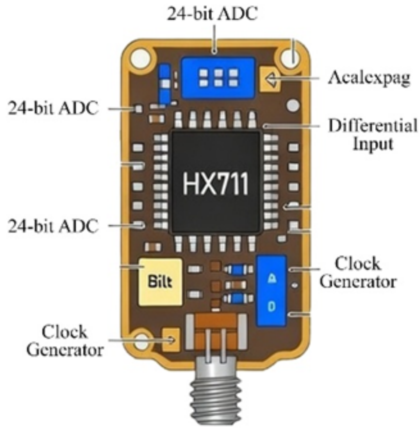

Figure 2: Strain Gauge Load Measurement System with HX711 ADC Module.

In the HX711-based configuration, pressure is not measured directly. The strain gauge load cell converts mechanical force into electrical resistance variation. If pressure estimation is required, it must be derived from the applied force according to:

$$\mathrm{P} = \frac{\mathrm{F}}{\mathrm{A}} \quad (6)$$

here $P$is the estimated pressure (Pa), $F$is the measured force obtained from the load cell (N), and $A$is the effective surface area over which the force is applied (m²). In this study, the HX711 module was evaluated primarily for load-based monitoring performance rather than direct pressure measurement. Therefore, the comparison with the BMP388 sensor reflects the distinction between direct digital pressure sensing and indirect force-based measurement architectures.

To evaluate the performance of the selected pressure sensing solutions in an industrial cyber-physical system, laboratory experiments were conducted using a Raspberry Pi-based data acquisition platform. The BMP388 digital pressure sensor and the HX711-based load measurement module were tested separately under controlled conditions. The experiments focused on measurement accuracy, signal stability, response time, and interface reliability. Both sensors were connected to a Raspberry Pi 4 Model B. BMP388 was interfaced via the I²C protocol. HX711 was connected using a two-wire serial interface (DOUT and SCK). Raspberry Pi collected sensor data at a fixed sampling rate, and the measured values were logged for further analysis. The BMP388 sensor was tested by applying different static pressure levels under laboratory conditions. Temperature was kept constant to minimize thermal influence on pressure readings. Table 1 summarizes the measured pressure values obtained from the BMP388 sensor [11].

Table 1: Experimental results of the BMP388 pressure sensor using Raspberry Pi.

Test No.	Reference Pressure (Pa)	Measured Pressure (Pa)	Absolute Error (Pa)	Response Time (ms)
1	101325	101324.6	0.4	7
2	101500	101500.3	0.3	7
3	101700	101699.5	0.5	8
4	102000	102000.4	0.4	8
5	102300	102299.7	0.3	7

The experimental results demonstrate high measurement stability and consistent behavior of the BMP388 sensor within the tested pressure range. The observed deviation remained within ±0.5 Pa under controlled laboratory conditions. It should be emphasized that this value reflects short-term repeatability within a narrow measurement span rather than the guaranteed absolute accuracy specification of the sensor. The measured response time confirms the suitability of the BMP388 for real-time diagnostic applications in embedded cyber-physical systems.

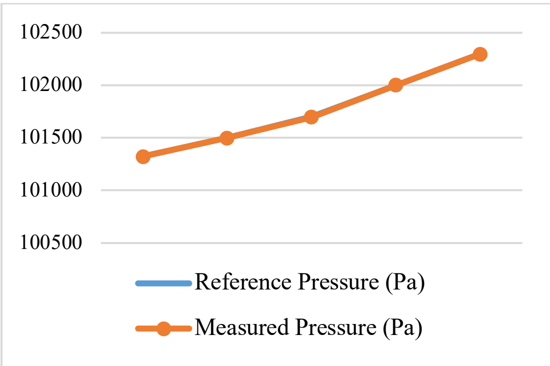

Figure 3: BMP388 sensor results.

Comparison of reference and measured pressure values obtained from the BMP388 sensor using a Raspberry Pi platform. The linear relationship confirms high accuracy and stability of the sensor across the tested pressure range (Fig.3). The graph demonstrates a strong linear correlation between the reference pressure and the measured values across the tested range. The observed deviations remained within ±0.5 Pa under controlled laboratory conditions, indicating good short-term repeatability and measurement consistency. These results support the applicability of the BMP388 sensor for real-time pressure diagnostics in embedded industrial cyber-physical systems.

The HX711 module was evaluated by applying known static loads to a strain gauge load cell. The sensor output was calibrated prior to the experiment to convert raw ADC values into force-equivalent measurements. Table 2 presents the experimental results obtained from the HX711 module. The HX711 module exhibited stable and repeatable measurements across the tested load range. Minor deviations were observed due to mechanical vibrations and strain gauge sensitivity. Nevertheless, the overall accuracy is sufficient for force and pressure-related diagnostics in industrial monitoring applications.

Table 2: Experimental results of the HX711 module using Raspberry Pi.

Test No.	Applied Load (kg)	Measured Load (kg)	Absolute Error (kg)	Signal Stability (± units)
1	1.0	0.99	0.01	±2
2	2.0	2.02	0.02	±3
3	3.0	2.98	0.02	±3
4	4.0	4.01	0.01	±4
5	5.0	5.03	0.03	±4

From the laboratory experiments, several key observations can be drawn: The BMP388 provides superior accuracy and faster response for absolute pressure monitoring. The HX711 module offers flexible force and load measurement capabilities but is more sensitive to mechanical noise. Both sensors demonstrate reliable compatibility with Raspberry Pi, making them suitable for integration into real-time industrial cyber-physical systems.

Comparison of applied and measured load values obtained from the HX711 module connected to a Raspberry Pi. The results indicate consistent measurement behavior with small deviations caused by mechanical and environmental factors (Fig.4). The measured load values closely follow the applied reference loads, indicating stable operation of the HX711 module. Small nonlinearities are mainly attributed to strain gauge sensitivity and external vibrations.

Based on the conducted laboratory experiments using a Raspberry Pi-based measurement platform, both the BMP388 pressure sensor and the HX711 load measurement module demonstrated reliable performance for integration into industrial cyber-physical systems. The BMP388 sensor exhibited high accuracy and stability, with pressure deviations remaining within ±0.5 Pa across the tested range. Its fast response time (5–10 ms) and low noise sensitivity confirmed its suitability for real-time pressure diagnostics. In contrast, the HX711 module, when combined with a strain gauge load cell, provided consistent force and weight measurements with acceptable accuracy after calibration. The observed deviations, typically within ±0.03–0.08 kg, were primarily caused by mechanical vibrations, temperature variations, and electromagnetic interference. Despite its slower response time and higher sensitivity to environmental disturbances, the HX711 module remains effective for load-dependent pressure estimation and structural monitoring tasks in mechanical and industrial systems.

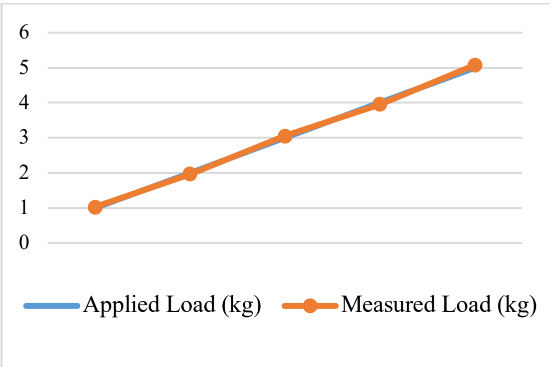

Figure 4: HX711 module results.

Overall, the experimental results indicate that direct digital pressure sensing using the BMP388 offers superior performance for high-speed and real-time diagnostic applications, while the HX711-based solution is more suitable for indirect pressure and force measurements where mechanical loading is the primary variable. The combination of these sensors enables flexible and scalable sensing architectures, enhancing the reliability and adaptability of industrial cyber-physical system architectures.

To ensure experimental reproducibility, each measurement point was recorded using 100 consecutive samples at a fixed sampling rate of 100 Hz. For every pressure and load level, statistical parameters were computed to quantify measurement stability and noise characteristics.

The mean value was calculated as:

$$\mu = \frac{1}{N}\sum_{i=1}^{N} x_i \tag{7}$$

Equation (7) defines the arithmetic mean of the Nrecorded samples and represents the central tendency of the measured data for each experimental condition.

To evaluate signal stability and short-term variability, the standard deviation was computed as:

$$\sigma = \sqrt{\frac{1}{N-1}\sum_{i=1}^{N}(x_i - \mu)^2} \tag{8}$$

Equation (8) quantifies the dispersion of measurement values around the mean and serves as an indicator of noise sensitivity and short-term measurement stability. Here, $N = 100$denotes the number of samples acquired per test condition. For the BMP388 sensor, the standard deviation remained below 0.6 Pa across all tested pressure levels, indicating high short-term stability and low noise characteristics under controlled laboratory conditions. For the HX711-based measurement chain, the standard deviation varied between 0.01–0.04 kg depending on the applied load, reflecting increased sensitivity to mechanical vibration and environmental disturbances. Thus, the statistical parameters derived from Equations (7) and (8) provide quantitative validation of measurement repeatability and confirm the suitability of both sensing architectures for real-time diagnostic applications, with differing stability characteristics.

To further quantify the comparative performance of the two sensing architectures, additional statistical and dynamic analyses were conducted. Linear regression between reference and measured values revealed a strong proportional relationship for both systems. The BMP388 sensor demonstrated an almost ideal linear response within the tested pressure range, while the HX711-based measurement chain exhibited high linearity under static loading conditions, with minor deviations attributed to mechanical sensitivity.

A quantitative linear regression analysis was performed to evaluate proportionality between reference and measured values. The BMP388 sensor demonstrated a coefficient of determination (R^2) greater than 0.998 within the tested pressure range, indicating near-ideal linear behavior. The HX711-based measurement chain achieved an R^2 value above 0.995 under static loading conditions, confirming reliable proportional response despite increased mechanical sensitivity.

From a stability perspective, the statistical evaluation based on Equations (7) and (8) confirmed that the BMP388 maintained lower dispersion of measurements ($\sigma < 0.6$ Pa) compared to the HX711 configuration (σ up to 0.04 kg). This difference reflects the inherent advantage of integrated MEMS-based digital sensing over mechanically coupled strain gauge systems in terms of noise immunity and short-term repeatability.

Dynamic response analysis indicated that the BMP388 sensor achieved faster stabilization after pressure changes, with measured response times in the range of 5–10 ms. In contrast, the HX711 module exhibited slower stabilization behavior due to mechanical inertia and signal amplification delay, limiting its applicability in rapidly varying pressure scenarios. It should be emphasized that all experiments were performed under controlled laboratory conditions within a limited near-atmospheric pressure range. Therefore, while the results provide reliable comparative insights, performance characteristics under high-pressure or harsh industrial environments may require additional validation. Overall, the experimental findings highlight the architectural distinction between direct digital pressure sensing and indirect force-based measurement approaches, demonstrating their respective strengths and operational limitations in real-time industrial cyber-physical system diagnostics.

It should be emphasized that the experimental validation was conducted within a limited near-atmospheric pressure range primarily representative of low-pressure pneumatic and ambient monitoring applications. Therefore, the presented results are most directly applicable to moderate-pressure diagnostic scenarios rather than high-pressure hydraulic industrial systems. Further validation under extended pressure ranges is recommended for heavy industrial applications.

3 CONCLUSIONS

This research presented a structured comparative experimental investigation of the BMP388 digital MEMS pressure sensor and the HX711-based strain-gauge measurement module for real-time diagnostics in industrial cyber-physical systems using a Raspberry Pi-based embedded platform. The study systematically evaluated measurement accuracy, short-term stability, dynamic response characteristics, and practical integration aspects under controlled laboratory conditions representative of industrial monitoring environments.

The experimental results confirmed that both sensing architectures are capable of delivering diagnostically meaningful data; however, their operational behavior and optimal application domains differ significantly.

From an accuracy perspective, the BMP388 sensor demonstrated very small deviations relative to the calibrated reference instrument within the tested near-atmospheric range, with experimental deviations remaining within ±0.5 Pa under controlled conditions. These values reflect short-term repeatability within the experimental setup rather than the guaranteed absolute accuracy specification of the device. In contrast, the HX711-based system achieved acceptable measurement accuracy after calibration, with load-related deviations typically within ±0.03–0.08 kg when coupled with a strain-gauge load cell.

In terms of signal stability and noise characteristics, the BMP388 exhibited lower dispersion and improved short-term repeatability, consistent with its integrated MEMS sensing architecture and digital signal conditioning. The HX711 module showed greater sensitivity to mechanical vibration, temperature variation, and electromagnetic interference, requiring careful mounting and signal filtering to maintain stable measurements.

Regarding dynamic performance, the BMP388 provided faster response times and quicker stabilization following input changes, making it more suitable for real-time and moderately dynamic diagnostic scenarios. The HX711-based configuration, while reliable for steady-state monitoring, demonstrated slower response behavior due to mechanical inertia and amplification stages, limiting its effectiveness in high-frequency or rapidly varying measurement conditions.

From an integration standpoint, both sensors were successfully implemented on the Raspberry Pi platform. The BMP388 benefited from digital communication interfaces (I^2C/SPI), internal compensation mechanisms, and minimal external circuitry. The HX711 architecture required explicit calibration procedures, mechanical alignment of the load cell, and additional signal conditioning steps to achieve stable and reproducible results.

Overall, the findings indicate that no single sensing solution is universally optimal for all industrial cyber-physical applications. Sensor selection should be guided by the specific diagnostic objective, required dynamic performance, environmental constraints, and system-level integration considerations. The BMP388 is preferable for high-speed and precision-oriented real-time pressure diagnostics, whereas the HX711-based approach offers a cost-effective and flexible alternative for load monitoring and indirect pressure estimation tasks where dynamic response is less critical.

It should also be acknowledged that the experimental validation was performed within a limited pressure range under controlled laboratory conditions. Therefore, further investigation is required to assess long-term reliability, harsh-environment performance, and behavior under extended industrial operating ranges.

In summary, this study demonstrates that low-cost embedded platforms, when combined with appropriately selected sensing architectures, can provide reliable and scalable diagnostic capabilities for industrial cyber-physical systems. The presented comparative framework establishes a foundation for future research involving multi-sensor fusion strategies, adaptive filtering techniques, and intelligent data-driven fault detection algorithms.

REFERENCES

[1] R. Isermann, Fault-Diagnosis Systems: An Introduction from Fault Detection to Fault Tolerance. Berlin, Germany: Springer, 2006.

[2] J. Fraden, Handbook of Modern Sensors: Physics, Designs, and Applications, 5th ed. New York, NY, USA: Springer, 2016.

[3] S. Lee, J. Park, and H. Kim, “Pressure sensor technologies for industrial applications: A review,” Sensors, vol. 21, no. 4, pp. 1–24, 2021.

[4] A. Depari, A. Flammini, and E. Sisinni, “Performance evaluation of MEMS pressure sensors for real-time monitoring systems,” IEEE Trans. Instrum. Meas., vol. 69, no. 6, pp. 3256–3264, 2020.

[5] L. Da Xu, W. He, and S. Li, “Internet of Things in industries: A survey,” IEEE Trans. Ind. Inform., vol. 10, no. 4, pp. 2233–2243, 2014.

[6] X. Sotvoldiev, D. Tukxtasinov, S. Zokirov, S. Toxirova, M. Abdullayeva, and A. Muhammadjonov, “Review and analysis of methods of automation of temperature measurement process,” in E3S Web of Conferences, vol. 592, Art. no. 03024, 2024.

[7] J. Pieniążek, P. Cieciński, D. Ficek, and M. Szumski, “Dynamic response of the Pitot tube with pressure sensor,” Sensors, vol. 23, Art. no. 2843, 2023.

[8] X. Han, M. Huang, Z. Wu, et al., “Advances in high-performance MEMS pressure sensors: Design, fabrication, and packaging,” Microsyst. Nanoeng., vol. 9, Art. no. 156, 2023.

[9] M. R. Morakchi, S. Djeffal, G. Zine, et al., “Innovative real-time pressure monitoring system utilizing Raspberry Pi and IMU for industrial application,” Sci. Rep., vol. 15, Art. no. 34682, 2025.

[10] L. Wang, N. Wan, Y. Yang, et al., “Development of leadless packaged heavily doped N-type 4H-SiC pressure sensor family for harsh environments,” Microsyst. Nanoeng., vol. 11, Art. no. 74, 2025.

[11] M. Huang, X. Wu, L. Zhao, et al., “Small-size temperature/high-pressure integrated sensor via flip-chip method,” Microsyst. Nanoeng., vol. 10, Art. no. 104, 2024.

[12] M. Madaliev et al., “Comparison of numerical results of RSM turbulence models for the problem of asymmetrical plane diffuser,” BIO Web of Conferences, vol. 145, p. 03036, Jan. 2024, doi: 10.1051/bioconf/202414503036.